

ASUTOSH COLLEGE



DEPARTMENT OF PHYSICS

Computational investigation of Allen-Cahn and Cahn-Hilliard equations

By
Sutirtha Paul

Under the supervision of:
Dr. Amit Kumar Bhattacharjee

July, 2021

Contents

List of Figures	3
List of Tables	3
1 Introduction	4
1.1 Thermodynamic Equilibrium and Phase transitions	4
1.1.1 Phase Transitions	4
1.2 Diffuse Interface theory	5
1.3 Allen-Cahn Equation	5
1.4 Cahn-Hilliard Equation	6
2 Numerical Methods	7
2.1 Non-dimensionalisation	7
2.1.1 Non-dimensionalisation of free energy	7
2.1.2 Non-dimensionalisation of equations	7
2.2 Spatial Methods	8
2.2.1 Finite Difference Methods	8
2.2.2 Pseudo-spectral Methods	9
2.2.3 Implementation	9
2.3 Temporal Methods	11
3 Implementation	13
3.1 One Dimension	13
3.1.1 Analytical Method	13
3.1.2 Numerical Results	13
3.2 Two dimensions	13
4 Conclusion and future work.	16
A Structure factor and correlation function	17
A.1 Non-uniform discrete Fourier transform	17
A.2 Structure factor	18

<i>CONTENTS</i>	2
B Cahn-Hilliard equation	20
B.1 One Dimension	20
B.2 Two Dimension	20
Bibliography	22

List of Figures

2.1	<i>Convergence of the derivative of some functions using Chebyshev Spectral method. The error is given by the L_2 norm of the difference between the calculated and the analytical result. At around 10^{-14} round-off errors take over leading to decrease in accuracy.</i>	10
3.1	<i>(a) The variation of error (L_2 norm) with system size N for both finite difference and Chebyshev spectral methods for the Allen-Cahn equation. The inset figure shows the tan hyperbolic interface at steady state. (b) The energy evolution of the system with time. ϵ is 0.01 and the system size is 64.</i>	14
3.2	The evolution of a system under the Allen-Cahn equation. The initial condition is completely random and slowly the system seperates into two phases.	15
A.1	Graph for structure factor	18
B.1	The variation of error (L_2 norm) with system size N for both finite difference and Chebyshev spectral methods for the Cahn-Hilliard equation. The inset figure shows the tan hyperbolic interface at steady state. ϵ is 0.2 and the system size is 64.	21

List of Tables

A.1	<i>Table of Length scale values with associated standard deviations. As can be seen the standard deviations are too high compared to the variaton in length scales to provide any meaningful graph or result.</i>	18
-----	---	----

Chapter 1

Introduction

In the following report we will be studying the Chebyshev spectral method for solving spatio-temporal equations. Particularly we will consider the case of the nonconservative Allen-Cahn equation and the conservative Cahn-Hilliard equation. We start with a review of phase transitions and the parameters used to define them, and then look at diffuse interface theory where the two equations originated.

1.1 Thermodynamic Equilibrium and Phase transitions

A system is defined to be in equilibrium when there is no tendency for the system to change state i.e. it is in mechanical, chemical and thermal equilibrium. A system in thermodynamic equilibrium can be completely characterised by its macroscopic properties and thus follow a defined set of rules which govern the change in various variables. To mathematically describe a system in thermodynamic equilibrium, we require thermodynamic potentials i.e. functions whose extremisation give the state of equilibrium. One such potential is the Helmholtz free energy can be defined as $F = U - TS$, where U represents the internal energy, T the temperature and S is the entropy of the system. The Helmholtz free energy represents the amount of energy available in the system that can be converted to work.

1.1.1 Phase Transitions

A phase transition occurs when a substance transitions from one thermodynamically distinct phase to the other. Ehrenfest classified the phase transitions on the basis of the properties of the derivatives of the system's free energy. If the first derivative is discontinuous at transition it is called a *first order* transition. If the second derivative is discontinuous it is known as a *second order* transition and so on. The point in the phase diagram where a phase equilibrium curve ends is known as the *critical point*. The corresponding temperature and pressure are known as the *critical temperature*

and *critical pressure*. The transition between an ordered and unordered phase can be characterised an order parameter. Each phase is characterised by a particular value of the order parameter.

1.2 Diffuse Interface theory

Next we consider the interface in a binary system. The interface can be between two different materials or between two phases of the same material. There can be two different approaches to modelling interfaces.

- Assuming a 'sharp' interface between the two materials i.e. a surface with zero thickness.
- Assuming a diffuse interface i.e. a surface of finite thickness.

Gibbs was the first to describe equilibrium thermodynamics for interfaces by assuming a 'sharp' surface and constructing a quantity called the surface excess ϕ_s . For the diffuse interface approach, two such surfaces are considered with a finite volume between them. This thus allows to work with extensive variables in the interfacial region.

Diffuse Interface theory was developed first to study behaviour near the critical point. Depending on the type of system, different quantities can function as the order parameter. For a system with different phases, a phase field variable ϕ conveniently functions as the order parameter. The phase field variable ϕ has the property of having a value of +1 in one ordered phase and -1 in the unordered phase. In the interfacial region ϕ varies smoothly. See [5] for a review.

1.3 Allen-Cahn Equation

The interfacial region contains a mixture of both phases. Thus the concentration of both substances is non-uniform in this region. In [3] Cahn and Hilliard showed that the free energy for such a non-uniform region can be expressed (to a first approximation) as the sum of the free energy of the homogenous system, which is a function of the long range order parameter and a gradient term, which is a function of the local composition.

$$F = \int F_o(\phi) + \frac{1}{2}c(\nabla\phi)^2 dV \quad (1.1)$$

Here we consider second order phase transitions. Since a second order transition is symmetric under time reversal, the free energy must remain invariant under the transformation $\phi \rightarrow -\phi$. Thus the free energy will contain only even power terms. Further the equilibrium order parameters will be of equal and opposite sign. Thus the potential has the double-well form given by:

$$F_o = \frac{1}{2}a\phi^2 - \frac{1}{4}b\phi^4 \quad (1.2)$$

If the order parameter is not a conserved quantity and the free energy is not at a minimum then Allen and Cahn postulated in [2] the change in order parameter is given by

$$\frac{\partial \phi}{\partial t} = -\Gamma \frac{\delta F}{\delta \phi} \quad (1.3)$$

This is known as the Allen-Cahn equation. Using the form of the free energy for second order transition we obtain:

$$\frac{\partial \phi}{\partial t} = \Gamma(a\phi - b\phi^3 + c\nabla^2 \phi) \quad (1.4)$$

Now at the boundary, we impose the no flux condition that is $\frac{\partial \phi}{\partial \mathbf{n}} = 0$ with the initial condition given by $\phi(x, 0) = \phi(x)$. This is also known as model A dynamics and describes the slow dynamics of a non-conservative variable.

1.4 Cahn-Hilliard Equation

If the order parameter is a conserved quantity then from Fick's laws of diffusion:

$$J = -D\nabla \mu \quad (1.5)$$

and the continuity equation:

$$\frac{\partial \phi}{\partial t} + \nabla \cdot J = 0 \quad (1.6)$$

we get

$$\frac{\partial \phi}{\partial t} = D\nabla^2 \mu \quad (1.7)$$

The chemical potential, μ is obtained from the free energy by $\mu = \frac{\delta F}{\delta \phi}$. Using the form of the free energy for a second order transition given in (1.2) we obtain:

$$\frac{\partial \phi}{\partial t} = D\nabla^2(b\phi^3 - a\phi - c\nabla^2 \phi) \quad (1.8)$$

We use the same Neumann conditions as above with $\frac{\partial \phi}{\partial \mathbf{n}} = 0$ and the initial condition given by $\phi(x, 0) = \phi(x)$

This is known as model B dynamics and describes the purely dissipative dynamics of a conserved variable.

Chapter 2

Numerical Methods

2.1 Non-dimensionalisation

2.1.1 Non-dimensionalisation of free energy

We use the form of the free energy for second order transition:

$$F_o = \frac{1}{2}a\phi^2 - \frac{1}{4}b\phi^4 \quad (2.1)$$

For non-dimensionalisation we pick the value of ϕ_0 which extremises the free energy. Solving the equation $\frac{\partial}{\partial \phi}(-\frac{1}{2}a\phi^2 + \frac{1}{4}b\phi^4) = 0$ (at steady state $\nabla \phi$ makes no contribution) gives us $\phi_0 = \pm \sqrt{\frac{a}{b}}$.

2.1.2 Non-dimensionalisation of equations

Allen-Cahn Equation

Using non-dimensionlised variable $\phi^* = \frac{\phi}{\phi_0}$ gives us:

$$\frac{\partial \phi^*}{\partial t} = \Gamma a(\phi^* - \phi^{*3} + \frac{c}{a}\nabla^2 \phi^*) \quad (2.2)$$

Using $\nabla^* = \sqrt{\frac{c}{a}}\nabla$, where $\sqrt{\frac{c}{a}}$ is the coherence length and using $t^* = (\Gamma a)t$ we get the non dimensionalised form of the Allen-Cahn equation:

$$\frac{\partial \phi^*}{\partial t^*} = \phi^* - \phi^{*3} + \nabla^{*2} \phi^* \quad (2.3)$$

Cahn-Hilliard Equation

Picking the same value for ϕ_0 as in the previous case and using $\phi^* = \frac{\phi}{\phi_0}$ we get:

$$\frac{\partial \phi^*}{\partial t} = \frac{Da^2}{c} \frac{c}{a} \nabla^2 (\phi^{*3} - \phi^* - \frac{c}{a} \nabla^2 \phi^*) \quad (2.4)$$

Using $\nabla^* = \sqrt{\frac{\varepsilon}{a}}\nabla$, where $\sqrt{\frac{\varepsilon}{a}}$ is the coherence length and using $t^* = \frac{Da^2}{c}t$ we get the non dimensionalised form of the Cahn-Hilliard equation:

$$\frac{\partial \phi^*}{\partial t^*} = \nabla^{*2}(\phi^{*3} - \phi^* - \nabla^{*2}\phi^*) \quad (2.5)$$

2.2 Spatial Methods

In this section we look at ways of handling the spatial part of spatio-temporal equations. The material is largely adapted from [6] and [7]. The key step is here is to approximate the unknown function as a sum of basis functions.

$$\phi(x) = \sum_{i=0}^k a_i u_i$$

The resulting polynomial is made to satisfy the differential equation at a number of chosen points to obtain the coefficients of expansion. The choice of basis functions is what separates the various methods.

2.2.1 Finite Difference Methods

In finite difference methods, a uniformly spaced grid $\{x_1, \dots, x_N\}$ with $x_j - x_i = h$ is considered. The basis functions are chosen to be low, fixed order polynomials, which satisfy the differential equation only in some sub interval. Thus the function is approximated by low order overlapping polynomials.

To approximate derivatives we make use of the second order finite difference approximation

$$\phi'(x_j) = \frac{\phi(x_{j+1}) - \phi(x_{j-1}))}{2h} \quad (2.6)$$

This can be written as a differentiation matrix given by

$$\begin{pmatrix} \phi'(x_0) \\ \vdots \\ \phi'(x_N) \end{pmatrix} = h^{-1} \begin{pmatrix} 0 & \frac{1}{2} & & & -\frac{1}{2} \\ -\frac{1}{2} & 0 & & & \\ & \cdot & \cdot & & \\ & & \cdot & \cdot & \cdot \\ & & & \cdot & 0 & \frac{1}{2} \\ \frac{1}{2} & & & -\frac{1}{2} & 0 \end{pmatrix} \begin{pmatrix} \phi(x_0) \\ \vdots \\ \phi(x_N) \end{pmatrix} \quad (2.7)$$

The matrix is sparse, which allows us to use high values of N. However the accuracy is limited due to the fixed order of the polynomials. Higher order polynomials suffer from being ill-conditioned when used over a equidistant grid.

2.2.2 Pseudo-spectral Methods

In pseudo-spectral methods, a set of points known as the Gauss-Chebyshev-Lobatto points (henceforth referred to as Chebyshev points) are used instead of equispaced points. The basis functions are the Chebyshev Polynomials, $T_n(\cos(\theta)) = \cos(n\theta)$ which are global basis functions i.e. they approximate the function over the entire interval compared to the local basis functions used in the finite difference method.

To approximate derivatives we consider the Chebyshev points, $x_j = \cos(j\pi/N)$. The differentiation matrix is given by a $(N+1) \times (N+1)$ matrix, D whose entries are given by:

$$D_{00} = \frac{2N^2 + 1}{6}, \quad D_{NN} = -\frac{2N^2 + 1}{6} \quad (2.8)$$

$$D_{jj} = -\frac{x_j}{2(1 - x_j^2)}, \quad j = 1, 2, \dots, N-1 \quad (2.9)$$

$$D_{ij} = \frac{c_i - 1}{c_j} \frac{(x_i - x_j)^{-1}}{x_i - x_j}, \quad i \neq j, \quad i, j = 1, 2, \dots, N-1 \quad (2.10)$$

where

$$c_i = \begin{cases} 2 & i = 0, N \\ 1 & \text{otherwise} \end{cases}$$

Compared to a finite difference matrix, this matrix is dense but the increased accuracy compensates for the additional computation cost.

Matrices for higher order derivatives are simply calculated by taking the corresponding power of the derivative matrix i.e. $\frac{d^2}{dx^2}$ is given by D^2 where D is the Chebyshev matrix defined above. To take the derivative of a multi-variable function, the partial derivative matrices are constructed by simply taking the kronecker product with the corresponding identity matrix i.e. $D_x = D \otimes I$ and $D_y = I \otimes D$. Higher dimensions or more variables can be calculated analogously.

The error in spectral methods decreases much faster than in finite difference method. This is because the order of spectral methods is not fixed. Thus as the number of points, N , increases not only do they become more closely spaced but unlike finite difference methods the order of the polynomials also increase. Spectral methods because of their high accuracy with a low number of points are thus known as memory-minimising methods.

2.2.3 Implementation

The chebyshev differentiation is implemented by directly computing (2.8) for the off diagonal elements. The diagonal elements are computed using the 'negative sum trick' which is given by:

$$D_{ii} = -\sum_{j=0}^N D_{ij} \quad (2.11)$$

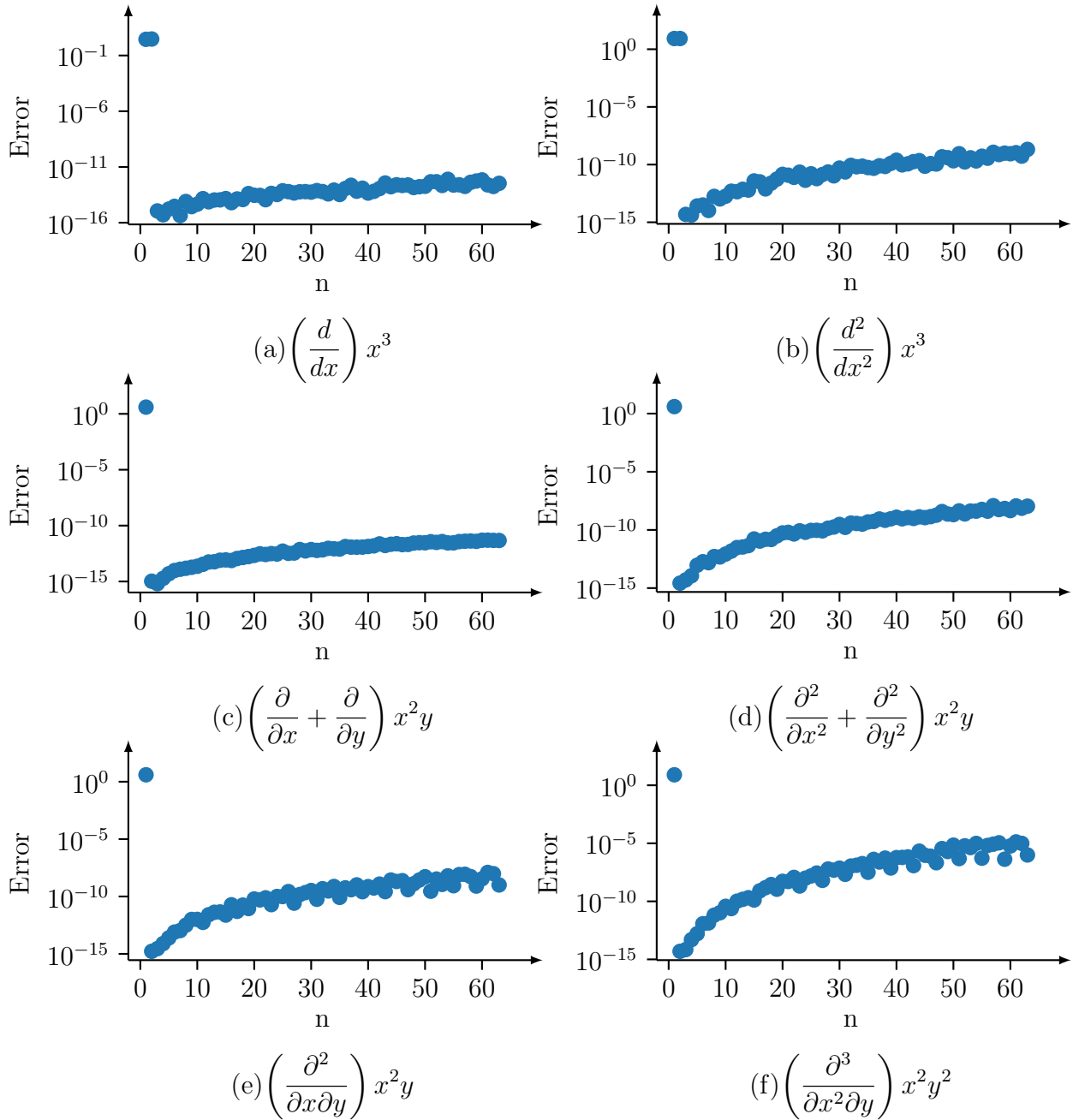


Figure 2.1: Convergence of the derivative of some functions using Chebyshev Spectral method. The error is given by the L_2 norm of the difference between the calculated and the analytical result. At around 10^{-14} round-off errors take over leading to decrease in accuracy.

This method of computing the matrix is more accurate than the other possible ways.[8]

2.3 Temporal Methods

For the temporal integration we use the fourth order Runge-Kutta method, henceforth known as RK4. The family of Runge-Kutta methods can be derived by approximating y_{n+1} by

$$y_{n+1} = y_n + ak_1 + bk_2 \quad (2.12)$$

where $k_1 = hf(x_0, y_0)$ and $k_2 = hf(x_0 + \beta k_1, x_n + \alpha h)$. If $k_2 = 0$ and $a = 1$ then it reduces to the simple euler method. We evaluate y_{n+1} to the order of $O(h^3)$ by considering the Taylor series for y :

$$y_{n+1} = y_n + hf(y_n, x_n) + \frac{h^2}{2} \left(\frac{\partial f}{\partial t} + f \frac{\partial f}{\partial y} \right) + O(h^3) \quad (2.13)$$

Expanding k_2 in (2.12) to $O(h^3)$ and using it in (2.12) we get

$$y_{n+1} = y_n + (a + b)hf(y_n, x_n) + bh^2 \left(\alpha \frac{\partial f}{\partial t} + \beta f \frac{\partial f}{\partial y} \right) (y_n, x_n) + O(h^3) \quad (2.14)$$

Comparing identical coefficients for (2.14) and equation 3 the value of a, b, α and β can be determined. This is the Runge-Kutta method of order 2 or RK2. Similarly RK4 can be derived by expanding and comparing the equations to $O(h^5)$. The equations for Rk4 are:

$$k_1 = hf(y_n, x_n) \quad (2.15)$$

$$k_2 = hf\left(y_n + \frac{k_1}{2}, x_n + \frac{h}{2}\right) \quad (2.16)$$

$$k_3 = hf\left(y_n + \frac{k_2}{2}, x_n + \frac{h}{2}\right) \quad (2.17)$$

$$k_4 = hf(y_n + k_3, x_n + h) \quad (2.18)$$

and finally

$$y_{n+1} = y_n + \frac{k_1 + 2k_2 + 2k_3 + k_4}{6} \quad (2.19)$$

The Runge-Kutta methods are explicit methods i.e. the state of the system at a later time is completely specified as a function of the system at previous time values.

Time step size

Equations with have a term which rapidly leads to variation of solutions are known as stiff equations. For such equations the use of explicit methods requires a rigid

bound on the time step. The CFL (Courant–Friedrichs–Lewy) condition provides such a condition requiring that in n -dimensions

$$\Delta t \left(\sum_{i=1}^n \frac{u_{x_i}}{\Delta x_i} \right) \leq C_{max} \quad (2.20)$$

Chapter 3

Implementation

3.1 One Dimension

3.1.1 Analytical Method

Here we consider the case with only one spatial dimension. We can obtain the steady state solution by considering the equation when it no longer varies with time, that is:

$$\frac{d^2\phi}{dx^2} = \phi^3 - \phi \quad (3.1)$$

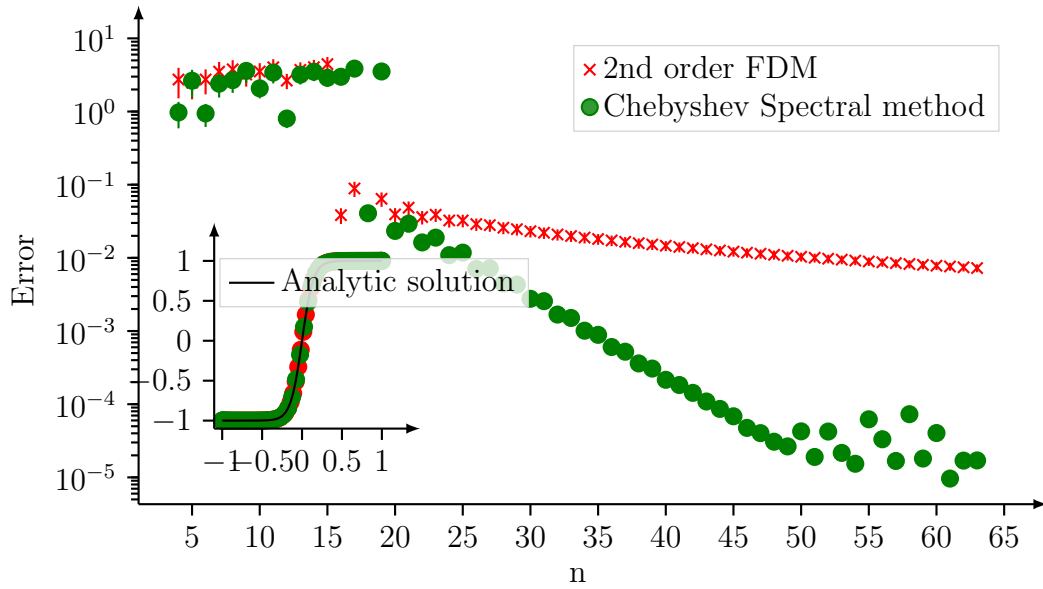
The solution to the above equation is $\tanh(\frac{x-x_0}{\xi})$ where $\xi = 2\epsilon$.

3.1.2 Numerical Results

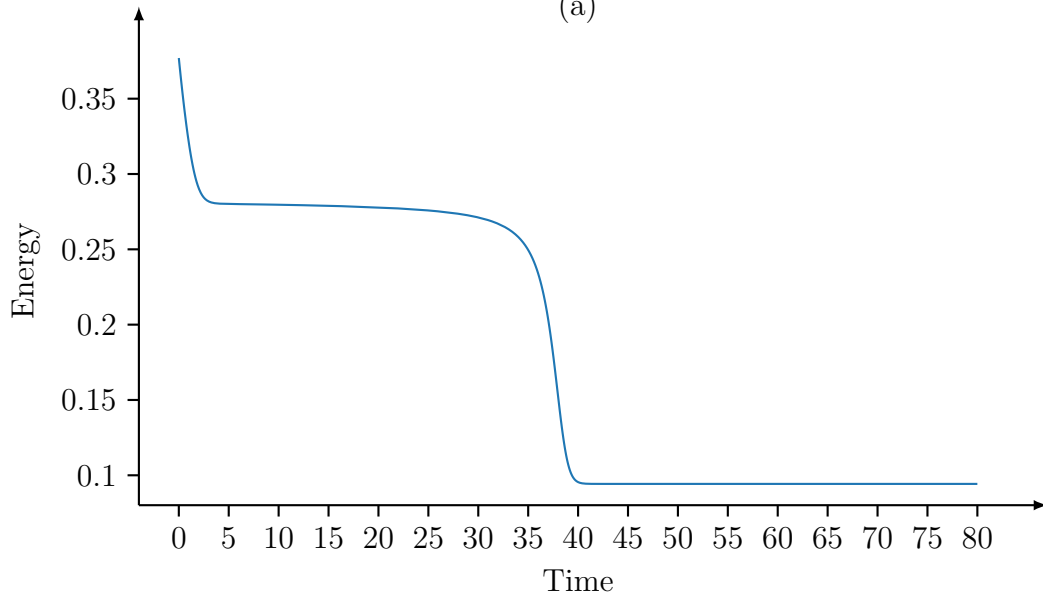
We use the chebyshev spectral method to discretise in one spatial dimension and use RK4 for the temporal part for both equations. As seen in the figure for Allen-Cahn, the error decreases much faster for Chebyshev spectral methods and accurate results can be obtained using systems of size 64. The accuracy is only limited by the fourth order time-stepping method.

3.2 Two dimensions

In two dimensions, for the Allen-Cahn equation we once again use the chebyshev spectral method for the two spatial dimensions and RK4 for the temporal part. We start with a $N \times N$ random grid and simulate the dynamics till it settles into two distinct states.



(a)



(b)

Figure 3.1: (a) The variation of error (L_2 norm) with system size N for both finite difference and Chebyshev spectral methods for the Allen-Cahn equation. The inset figure shows the tan hyperbolic interface at steady state. (b) The energy evolution of the system with time. ϵ is 0.01 and the system size is 64.

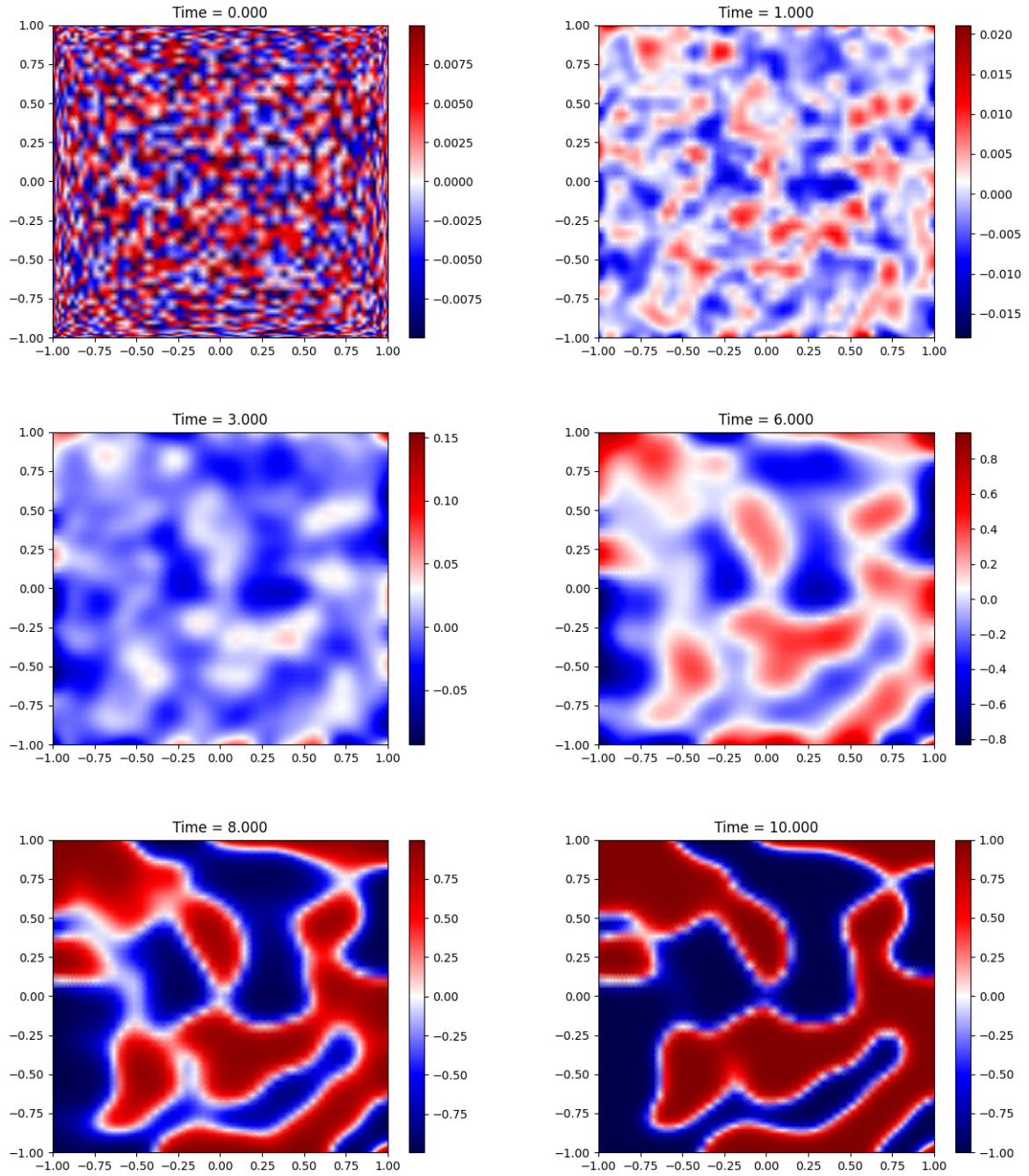


Figure 3.2: The evolution of a system under the Allen-Cahn equation. The initial condition is completely random and slowly the system separates into two phases.

Chapter 4

Conclusion and future work.

In this report we have shown that there are advantages to using pseudo-spectral methods over finite difference methods when solving partial differential equations. They converge faster and thus accurate results can be obtained with low values of N . However the choice of basis functions must be considered carefully, further experiments using other basis functions and other equations can give an idea of their limits and the suitability of each basis for different equations.

Finally, this work can simply be extended to three dimensions, which we could not carry out due to hardware restrictions. Since the method utilised here has been demonstrated to be working correctly for the Allen-Cahn equation, we can use it to investigate similar but more complicated systems.

Appendix A

Structure factor and correlation function

A good way of to check the validity of results is to calculate the functions $C(r, t)$ and $S(r, t)$ which are the angular averages of the correlation function

$$C(\mathbf{r}, t) = \frac{\int d^3\mathbf{x} \phi(\mathbf{x}, t) \phi(\mathbf{x} + \mathbf{r}, t)}{\int d^3x \phi(\mathbf{x}, t) \phi(\mathbf{x}, t)} \quad (\text{A.1})$$

and it's fourier transform, the structure factor, respectively.

$$S(\mathbf{k}, t) = \frac{\phi(\mathbf{k}, t) \phi(-\mathbf{k}, t)}{\int d^3\mathbf{k} \phi(\mathbf{k}, t) \phi(-\mathbf{k}, t)} \quad (\text{A.2})$$

where ϕ is the phase field variable. Hence, $C(r, t) = \sum_{|\mathbf{r}|=r} C(\mathbf{r}, t)$ and $S(r, t) = \sum_{|\mathbf{k}|=k} S(\mathbf{k}, t)$. Theoretically, these functions have the scaling form as $C(r, t) = F(r/L(t))$ and $S(k, t) = L^d G[kL(t)]$. The length is calculated from the structure factor as

$$< k >^2 = \frac{1}{L(t)^2} = \frac{\sum_{\mathbf{k}} k^2 S(\mathbf{k}, t)}{\sum_{\mathbf{k}} S(\mathbf{k}, t)} \quad (\text{A.3})$$

Since we are working with Chebyshev points, which are non-equispaced we need to calcute an unequally spaced fourier transform. Simply interpolating to an equispaced grid limits the accuracy of the results as they are now bounded by figure the accuracy of the interpolating algorithm.

A.1 Non-uniform discrete Fourier transform

The basic formula for a non-uniform discrete fourier transform simply follows from the equispaced one. It is given by

$$X_k = \sum_{n=0}^{N-1} x_n e^{-2\pi i p_n f_k} \quad (\text{A.4})$$

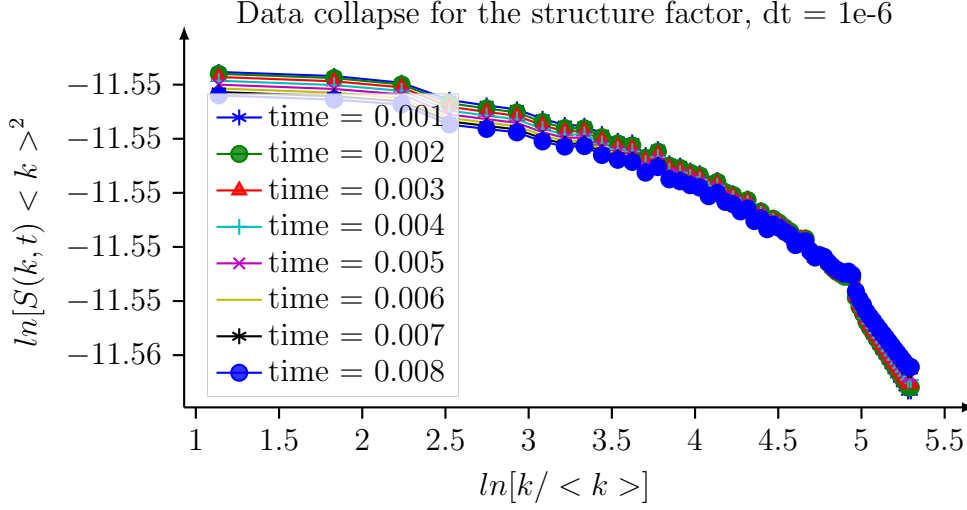


Figure A.1: Graph for structure factor

where p_n are the sample points and f_k are the frequencies at which the DFT is computed. The frequencies f_k are taken as $f_k = -\frac{2}{N}x_k$. [10]

A.2 Structure factor

An attempt to calculate the structure factor from the calculated data for the 2D Allen-Cahn equation led to the above figure. The data is averaged over 100 different initial conditions. An estimate of the length scale can also be obtained by taking the inverse of the expectation value as in equation However, when we calculate the length scale it turns out to have a large standard deviation, which proves many more iterations are needed and the graph for structure factor is also not accurate. The correlation

t	L(t)	Standard Deviation
0.001	202.769	0.210
0.002	202.766	0.179
0.003	202.762	0.160
0.004	202.759	0.146
0.005	202.756	0.137
0.006	202.753	0.130
0.007	202.750	0.124
0.008	202.747	0.120

Table A.1: Table of Length scale values with associated standard deviations. As can be seen the standard deviations are too high compared to the variation in length scales to provide any meaningful graph or result.

function can also be calculated with the above data, but it requires taking the inverse fourier transform of the structure factor.

Appendix B

Cahn-Hilliard equation

For the Cahn-Hilliard equation a similar approach to Allen-Cahn was attempted. The spatial dimension was resolved with the chebyshev spectral methods while the temporal dimension was computed using RK4. The Cahn-Hilliard equation is a stiff equation and using an explicit integrator like RK4 thus requires time steps of $\sim (\Delta x)^4$.

B.1 One Dimension

We obtained the following graph on solving the Cahn-Hilliard to get the tan hyperbolic interface. Note that there is not much difference between the Chebyshev and the finite difference methods. This is due to finite precision effects for polynomial expansion which occurs due to the fourth power of the expansion. For higher derivatives, the error increases with N leading to wildly inaccurate results.[\[9\]](#).

Thus a different set of basis functions need to be chosen to obtain accurate results.

B.2 Two Dimension

For two dimensions, the nature of the equation - it evolves slowly and then speeds up, requires a large computation time since we're using an explicit integrator with uniform time stepping. This was prohibitive with the available hardware but a similar approach should work. An adaptive time stepping solution is also possible.[\[11\]](#)

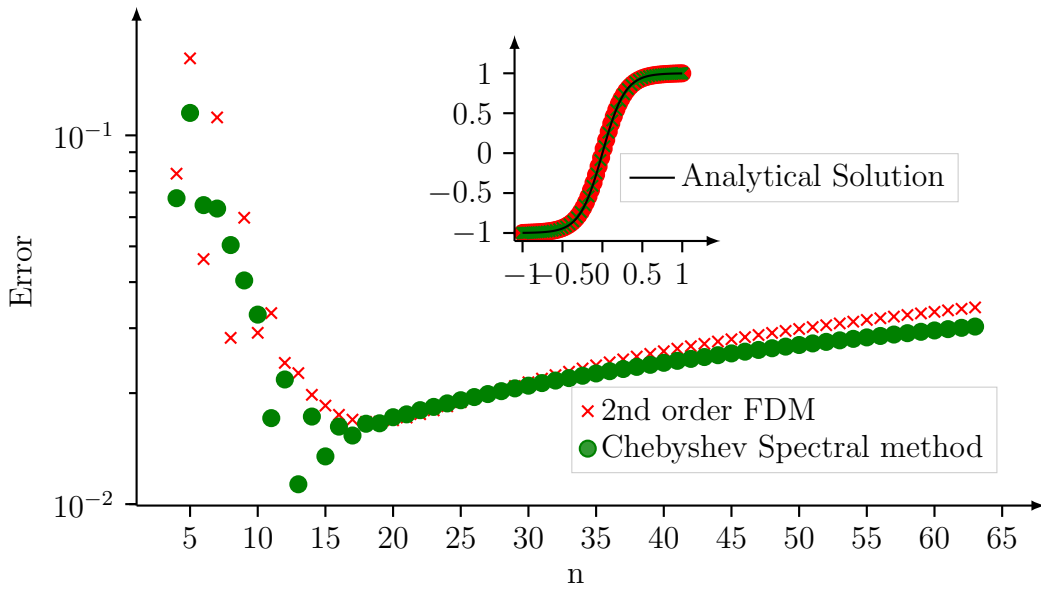


Figure B.1: The variation of error (L_2 norm) with system size N for both finite difference and Chebyshev spectral methods for the Cahn-Hilliard equation. The inset figure shows the tan hyperbolic interface at steady state. ϵ is 0.2 and the system size is 64.

Bibliography

- [1] P.M. Chaikin and T.C. Lubensky, *Principles of Condensed Matter Physics*, Cambridge University Press, 1995.
- [2] S. M. Allen and J. W. Cahn, *A microscopic theory for antiphase boundary motion and its application to antiphase domain coarsening*, Acta Metallurgica, 27 (1979), 1085–1095.
- [3] J. W. Cahn and J. E. Hilliard, *Free energy of a nonuniform system. I. Interfacial free energy*, J. Chem. Phys., 28 (1958), 258–267.
- [4] Heike Emmerich *The Diffuse Interface Approach in Materials Science*, Springer-Verlag Berlin Heidelberg, 2003
- [5] D.M. Anderson, G.N. Mcfadden and A.A. Wheeler, *Diffuse-interface methods in fluid mechanics* Annu. Rev. Fluid Mech., 30 (1998), 139–165
- [6] Lloyd N. Trefethen, *Spectral Methods in MATLAB*, Society for Industrial and Applied Mathematics, 2000
- [7] John P. Boyd, *Chebyshev and Fourier Spectral Methods*, 2nd Edition, Dover Publications, 2000
- [8] R. Baltensperger and M. Trummer, *Spectral Differencing with a Twist*, SIAM J. Sci. Comput., 24 (2003), 1465-1487
- [9] J. Hesthaven, S. Gottlieb and D. Gottlieb, *Spectral Methods for time dependent problems*, Cambridge University Press, 2007.
- [10] A. Dutt and V. Rokhlin, *Fast Fourier Transforms For Nonequispaced Data*, SIAM J. Sci. Comput., 14 (1993), 1368-1393
- [11] A. Christlieb, J. Jones, K. Promislow, B. Wetton, M. Willoughby, *High accuracy solutions to energy gradient flows from material science models*, J. Comp. Phys., 257 (2014), 193-215